INSTITUTE OF PHYSICS PUBLISHING PHYSICS IN MEDICINE AND BIOLOGY

Phys. Med. Biol. **49** (2004) 2799–2809 PII: S0031-9155(04)67594-4

Neural attractor network for application in visual field data classification

Wolfgang Fink

Doheny Eye Institute, Keck School of Medicine at the University of Southern California, Los Angeles, CA 90033, USA
and
California Institute of Technology, Pasadena, CA 91125, USA

E-mail: wfink@krl.caltech.edu

Received 14 August 2003
Published 11 June 2004
Online at stacks.iop.org/PMB/49/2799
doi:10.1088/0031-9155/49/13/003

Abstract

The purpose was to introduce a novel method for computer-based classification of visual field data derived from perimetric examination, that may act as a 'counsellor', providing an independent 'second opinion' to the diagnosing physician. The classification system consists of a Hopfield-type neural attractor network that obtains its input data from perimetric examination results. An iterative relaxation process determines the states of the neurons dynamically. Therefore, even 'noisy' perimetric output, e.g., early stages of a disease, may eventually be classified correctly according to the predefined idealized visual field defect (scotoma) patterns, stored as attractors of the network, that are found with diseases of the eye, optic nerve and the central nervous system. Preliminary tests of the classification system on real visual field data derived from perimetric examinations have shown a classification success of over 80%. Some of the main advantages of the Hopfield-attractor-network-based approach over feed-forward type neural networks are: (1) network architecture is defined by the classification problem; (2) no training is required to determine the neural coupling strengths; (3) assignment of an auto-diagnosis confidence level is possible by means of an overlap parameter and the Hamming distance. In conclusion, the novel method for computer-based classification of visual field data, presented here, furnishes a valuable first overview and an independent 'second opinion' in judging perimetric examination results, pointing towards a final diagnosis by a physician. It should not be considered a substitute for the diagnosing physician. Thanks to the worldwide accessibility of the Internet, the classification system offers a promising perspective towards modern computer-assisted diagnosis in both medicine and tele-medicine, for example and in particular, with respect to non-ophthalmic clinics or in communities where perimetric expertise is not readily available.

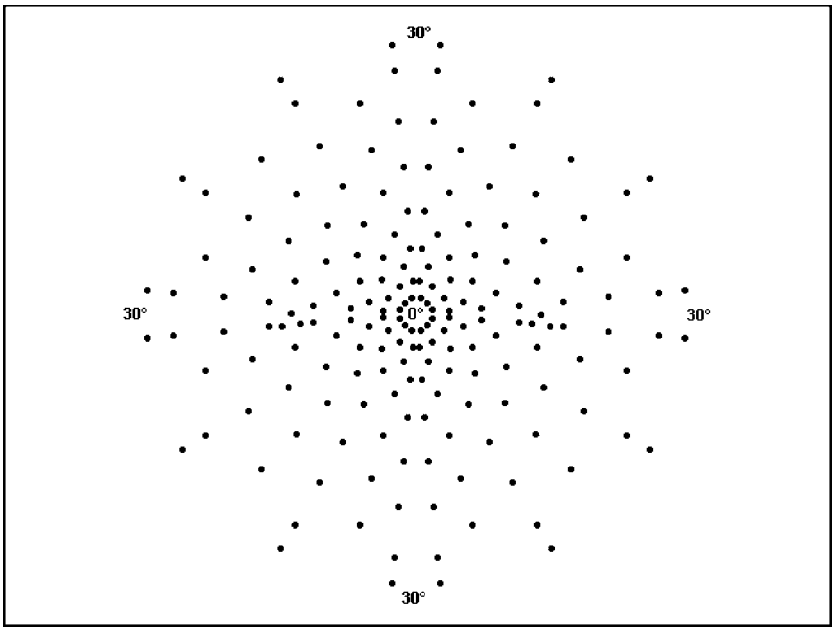

Figure 1. Spatial arrangement of the 190 eccentric test locations used by the TAP (by Oculus Optikgeräte GmbH) for the central 30° of the visual field, radially from the centre of fixation. There is a total of 191 test locations, including the centre of fixation not depicted here.

1. Introduction

What is *perimetry*? Perimetry, or visual field testing, has always been an important part of an ophthalmological evaluation since it comprises a large part of a person's visual function. Perimetry is the systematic measurement of visual field function. The two most commonly used types of perimetry are *Goldmann kinetic perimetry* and *threshold static automated perimetry*. With *Goldmann or 'kinetic' perimetry*, a trained perimetrist moves the stimulus manually. The stimulus brightness is held constant. The spatial limits of the visual field are mapped to light stimuli of different sizes and brightness. With *threshold static automated perimetry*, the visual field examination is performed by computer programs. The most commonly used one tests the central 30° of the visual field, radially from the centre of fixation, using a variety of test location arrangements of light stimuli (figure 1 shows an arrangement of 190 eccentric test locations used by the Tübingen Automated Perimeter (TAP), see section 2). This is accomplished by keeping the size and location of a target constant and varying the brightness until the dimmest target the patient can see at each of the test locations is found, hence the name 'threshold static automated perimetry'. These maps of visual sensitivity, made by either of these methods, are important in diagnosing diseases of the visual system non-invasively. Different patterns of visual field loss are found with diseases of the eye, optic nerve and the central nervous system.

Since many ophthalmological and neuroophthalmological diseases and lesions, even subtle ones, may be recognized from perimetric examinations, the appropriate classification of visual field data is essential for diagnosis. Adequate classification and interpretation of perimetric examination results is not a trivial task and requires well-trained personnel with long-term experience.

There has been recent interest in computer-based classification systems for visual field data using different approaches, e.g., feed-forward networks and self-organizing (Kohonen) maps

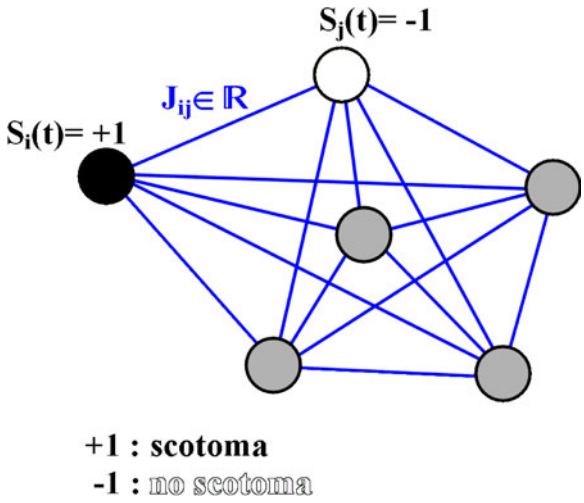

Figure 2. Hopfield-attractor network with $N = 6$ neurons. Each neuron is assigned to one tested stimulus location in the perimetric examination (see figure 1 for an example arrangement of stimulus locations).

(Kelman *et al* 1991, Nagata *et al* 1991, Keating *et al* 1992, 1993, Mutlukan and Keating 1994, Goldbaum *et al* 1994, Spenceley *et al* 1994, Henson *et al* 1996, 1997a, 1997b, Brigatti *et al* 1997). In the work presented here, an alternative kind of neural network is proposed, namely a Hopfield-attractor network (Hopfield 1982, Hertz *et al* 1991, Müller and Reinhardt 1990), for application in visual field data classification. It may be considered a 'counsellor' and not a substitute for the diagnosing physician, providing a valuable first overview and an independent 'second opinion' in judging perimetric examination results, pointing towards a final diagnosis by a physician. The data set on which the classification system operates on and classification results were already introduced at the 13th International Perimetric Society Meeting in Gardone Riviera, Italy, 1998 (Fink *et al* 1999). The paper presented here focuses on the mathematical underpinning rather than on the classification results obtained using the above-mentioned data set.

2. Methods

The classification system is based on a neural Hopfield-attractor network (see figure 2) that consists of N binary neurons. These neurons are assigned to the N stimulus locations of the stimulus grid that is used to examine the visual field, e.g., the TAP (by Oculus Optikgeräte GmbH) stimulus grid for the central 30°-visual field used here. Therefore, the neurons obtain their input data from perimetric examination results. We define '+1' as a scotoma (visual field defect) and '-1' as no scotoma at a particular test location within the visual field under examination.

It should be pointed out that this binary approach is a simplification, since in conventional automated threshold perimetry usually more than one luminosity class for the light stimuli (e.g., $1+6$ for the TAP) is used for detecting not only absolute but also relative scotomata. For the purpose of this study depending on a user-/examination-defined luminosity class threshold, all relative scotomata in a perimetric examination result above that threshold are considered absolute scotomata and the those below are omitted, i.e. considered 'normal' (see also sections 3 and 4). An example of this binary scotomata conversion is depicted in figures 3 and 4.

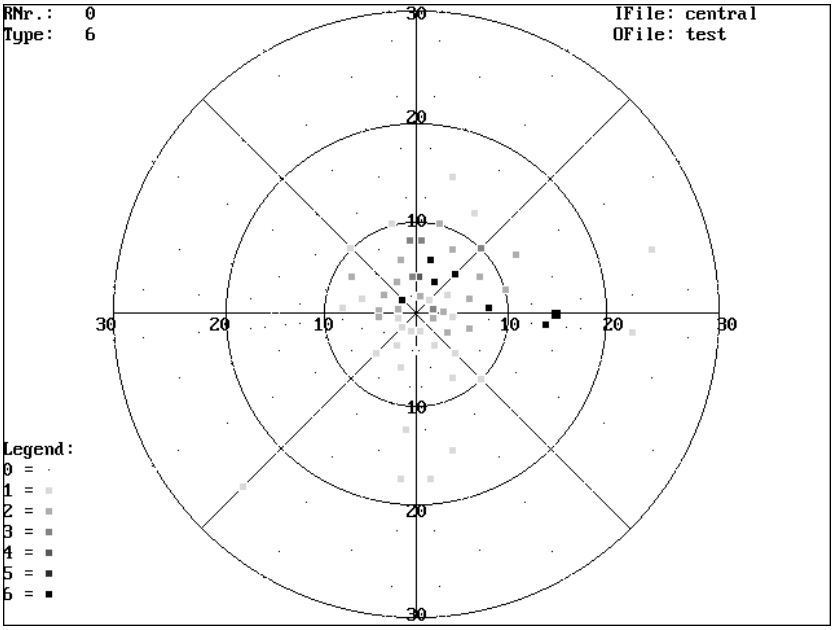

Figure 3. Initial neural network configuration: visual field data derived from a perimetric examination with, in this case, the TAP. Displayed are the 190 eccentric stimulus test locations and the resulting stimulus intensities recognized by the patient during the perimetric examination. For display purposes, the recognized stimulus intensities are encoded in grey scales (see legend in the figure at the lower left).

The N neurons are fully connected with each other via synaptic couplings J_{ij}. These synaptic coupling strengths can be calculated directly from the patterns to be stored as attractors of the network by means of, e.g., the *Hebb rule* or the *projection rule* (Hertz *et al* 1991, Müller and Reinhardt 1990). In the particular case of visual field data classification, the *attractors* are predefined idealized scotomata patterns such as hemianopic field defects, sectoral defects, central scotomata, para-central scotomata, centrocoecal scotomata, nerve fibre bundle defects, which are typically associated with diseases such as chiasmal and post-chiasmal lesions, glaucoma, geniculate lesions, maculopathies, optic neuropathies, paramacular processes (details provided in Schiefer and Wilhelm (1995)).

At the present stage of the classification system and for further simplification, each neuroophthalmological disease contained in the classification system is represented by one idealized scotomata pattern. Furthermore, only monocular perimetric examination results are considered (see also section 4).

2.1. Relaxation process

The following dynamic, iterative *relaxation process* determines the states $S_i(t)$ of the N neurons dynamically:

$$S_i(t+1) = \operatorname{sgn}(h_i(t) - \tilde{\vartheta}_i) = \operatorname{sgn}\left(\sum_{j=1}^{N} J_{ij} S_j(t) - \tilde{\vartheta}_i\right)$$

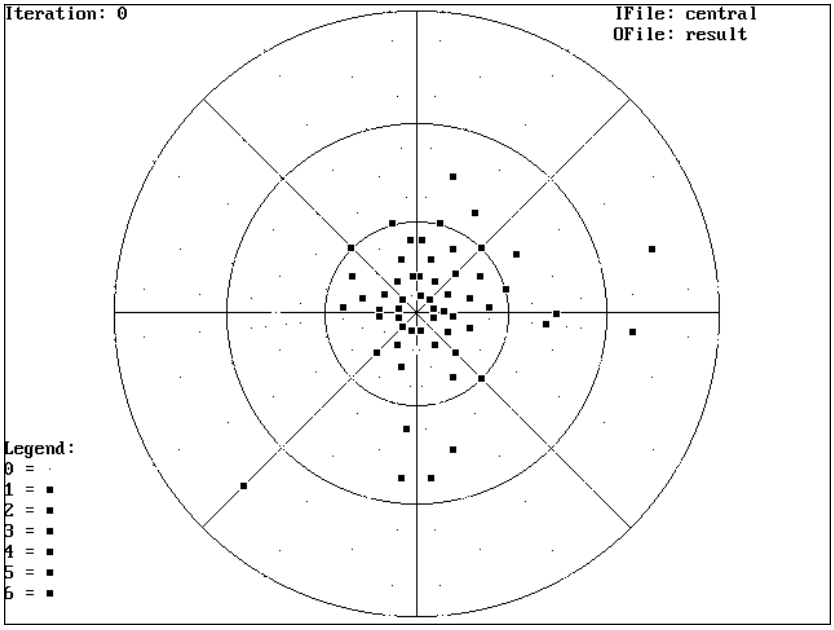

Figure 4. Initial neural network configuration: the relative scotomata, depicted in figure 2, are converted to a binary pattern according to a user-/examination-defined luminosity class threshold.

with

$$\operatorname{sgn}(x) = \begin{cases} +1: & x > 0 \\ -1: & \text{otherwise} \end{cases}$$

h_i = synaptic potential of ith neuron

$\tilde{\vartheta}_i$ = threshold of ith neuron.

Often the threshold $\tilde{\vartheta}_i$ is set to 0, which leads to

$$S_i(t+1) = \operatorname{sgn}\left(\sum_{j=1}^{N} J_{ij} S_j(t)\right).$$

Even 'noisy' perimetric output (see figures 3 and 4), e.g., early stages of a disease, may eventually be classified correctly (see figure 5) according to the predefined attractors of the network. 'Noisy' perimetric output means a scotomata pattern that differs from all attractors (idealized scotomata patterns) stored in the network. A *fixpoint* or attractor of the network dynamics is reached, if the condition $S_i(t+1) = S_i(t)$ is simultaneously fulfilled for each neuron i of the network.

2.2. Hebb's rule

One advantage of choosing a Hopfield-attractor network is that no learning process is required for determining the synaptic coupling strengths J_{ij}. Instead, these can be calculated directly from the idealized scotomata patterns $\vec{\sigma}^{\mu}$, $\mu = 1, \ldots, p$, which define the p attractors of the network and are represented as N-dimensional binary vectors:

$$J_{ij} := \frac{1}{N} \sum_{\mu=1}^{p} \sigma_i^{\mu} \sigma_j^{\mu} \qquad \forall i, j = 1, \ldots, N \qquad \sigma_i^{\mu}, \sigma_j^{\mu} \in \{-1, +1\}.$$

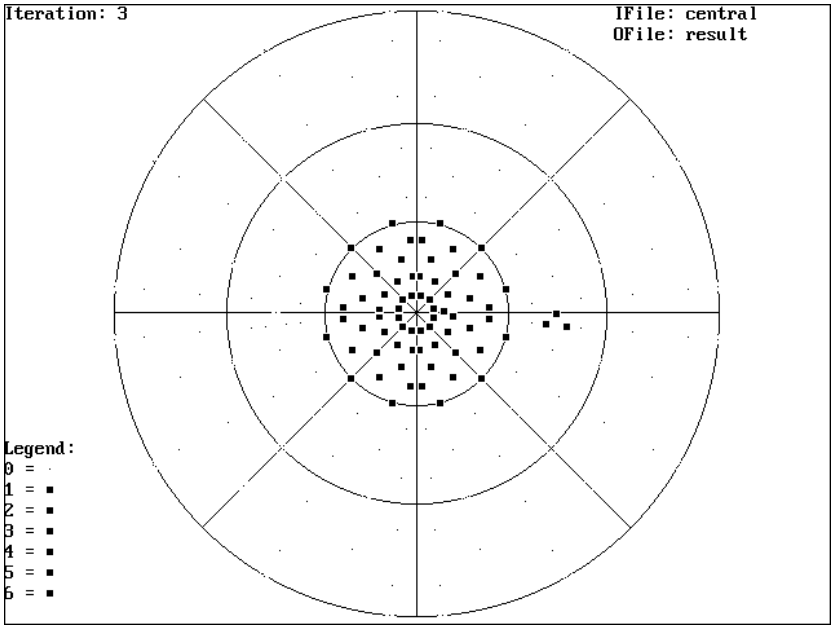

Figure 5. Final neural network configuration: fixpoint configuration of the network dynamic after the relaxation process of the Hopfield-attractor network.

This rule is usually referred to as *Hebb's rule*. It resolves the pattern storage problem as can be seen from the following (Hertz *et al* 1991, Müller and Reinhardt 1990):

$$\begin{aligned} h_i^{(\nu)} &= \sum_{j=1}^{N} J_{ij}\sigma_j^{\nu} \\ &= \frac{1}{N}\sum_{\mu=1}^{p}\sigma_i^{\mu}\sum_{j=1}^{N}\sigma_j^{\mu}\sigma_j^{\nu} \\ &= \frac{1}{N}\left[\sigma_i^{\nu}\sum_{j=1}^{N}\underbrace{\sigma_j^{\nu}\sigma_j^{\nu}}_{=1} + \sum_{\mu\neq\nu}\sigma_i^{\mu}\sum_{j=1}^{N}\sigma_j^{\mu}\sigma_j^{\nu}\right] \\ &= \sigma_i^{\nu} + \underbrace{\frac{1}{N}\sum_{\mu\neq\nu}\sigma_i^{\mu}\sum_{j=1}^{N}\sigma_j^{\mu}\sigma_j^{\nu}}_{\text{noise term}} \qquad \forall\nu = 1,\ldots,p. \end{aligned} \tag{1}$$

For large N and p it can be statistically shown that the noise term for uncorrelated patterns is typically of the order of $\sqrt{\frac{p-1}{N}}$. The smaller the so-called *storage capacity* $\alpha := \frac{p}{N}$ the bigger the likelihood that the νth pattern is a stable network configuration, hence a fixpoint or attractor of the network dynamics described above:

$$S_i^{(\nu)}(t=1) = \operatorname{sgn}\bigl(h_i^{(\nu)}(t=0)\bigr) = \operatorname{sgn}\bigl(\sigma_i^{\nu}\bigr) = \sigma_i^{\nu}.$$

If a 'noisy' pattern (visual field data derived from perimetric examination) differs in n test locations from an attractor stored in the network, it might still be classified correctly within one global update of all N neurons under the condition $n, p \ll N$. However, if the number

p of stored idealized scotomata patterns (attractors) is comparable to the total number of neurons N, these patterns cannot be recalled reliably. With methods of *statistical mechanics* it is possible to calculate the *critical storage capacity* $\alpha_c := \frac{p_c}{N}$ in the *thermodynamic limit* $N \longrightarrow \infty$ for finite $\frac{p}{N}$ and for independent and randomly chosen attractors (Hertz *et al* 1991, Müller and Reinhardt 1990): $\alpha_c \approx 0.138$.

For $\alpha < \alpha_c$, a reliable recall of random and independent attractors is possible. Above α_c a *discontinuous phase transition* from perfect recall of the stored patterns to total confusion occurs. The reason for this is the noise term in equation (1), caused by the correlations within the pattern set to be stored as attractors of the network.

2.3. Projection rule: storing correlated patterns

The problem of correlations within the pattern set to be learned may be overcome by the so-called *projection rule* (Hertz *et al* 1991, Müller and Reinhardt 1990) that allows us to store up to $p = N$ ($\alpha = 1$) arbitrarily correlated patterns under the only condition that the patterns are linearly independent. Defining

$$Q_{\mu\nu} := \frac{1}{N}\sum_{i=1}^{N}\sigma_i^\mu\sigma_i^\nu \qquad 1 \leqslant \mu, \nu \leqslant p$$

as the square matrix $\underline{\underline{Q}}$ of the pairwise scalar products of all patterns, it follows from the linear independence of the patterns that $\underline{\underline{Q}}$ is invertible. Therefore, the new synaptic coupling strengths $\tilde{J}_{ij}$ read as follows:

$$\tilde{J}_{ij} := \frac{1}{N}\sum_{\mu,\nu}\sigma_i^\mu(Q^{-1})_{\mu\nu}\sigma_j^\nu \qquad \forall i, j = 1, \ldots, N.$$

This notation is similar to the notation of a projection operator, thus giving the projection rule its name. The following proof shows that the new couplings are also a solution of the pattern storage problem:

$$\begin{aligned}
\tilde{h}_i &= \sum_{j=1}^{N}\tilde{J}_{ij}\sigma_j^\lambda \\
&= \frac{1}{N}\sum_{\mu,\nu}\sigma_i^\mu(Q^{-1})_{\mu\nu}\sum_{j=1}^{N}\sigma_j^\nu\sigma_j^\lambda \\
&= \sum_{\mu,\nu}\sigma_i^\mu(Q^{-1})_{\mu\nu}Q_{\nu\lambda} \\
&= \sum_{\mu,\nu}\sigma_i^\mu\delta_{\mu\lambda} \qquad \text{with } \delta_{\mu\lambda} = 1, \text{if } \mu = \lambda; 0 \text{ otherwise} \\
&= \sigma_i^\lambda.
\end{aligned}$$

In contrast to the Hebb rule there is *no* noise term.

2.4. Classification confidence criteria: overlap parameter and Hamming distance

In the classification system presented here, two confidence criteria (Hertz *et al* 1991, Müller and Reinhardt 1990) for the classification of perimetric examination results are introduced:

Table 1. Classification result sorted in descending order of probability: visual field defect code (VFDC), overlap parameter and Hamming distance, before and after the relaxation process of the Hopfield-attractor network, respectively.

	Overlap		Hamming		
VFDC	Before	After	Before	After	Remarks
21	58.95%	93.68%	39	6	Nerve fibre bundle defects: centrocoecal scotomata
3	57.89%	56.84%	40	41	Central scotomata
4	43.16%	42.11%	54	55	Para-central scotomata: moved downwards
5	49.47%	42.11%	48	55	Para-central scotomata: moved upwards
7	30.53%	27.37%	66	69	Sectoral/wedge-shaped defects
8	38.95%	27.37%	58	69	Sectoral/wedge-shaped defects
13	38.95%	27.37%	58	69	Normal finding
18	36.84%	25.26%	60	71	Blind spot: dislocation and size change: strong hyperopia
6	27.37%	24.21%	69	72	Sectoral/wedge-shaped defects
9	23.16%	24.21%	73	72	Sectoral/wedge-shaped defects
10	29.47%	24.21%	67	72	Sectoral/wedge-shaped defects
11	40.00%	24.21%	57	72	Sectoral/wedge-shaped defects
12	29.47%	24.21%	67	72	Sectoral/wedge-shaped defects
15	37.89%	24.21%	59	72	Blind spot: rotated downwards
16	37.89%	24.21%	59	72	Blind spot: rotated upwards
14	31.58%	20.00%	65	76	Blind spot: change in size
19	31.58%	15.79%	65	80	Nerve fibre bundle defects: wedge-shaped scotomata
17	30.53%	12.63%	66	83	Blind spot: dislocation and size change: strong myopia
22	12.63%	3.16%	83	92	Hemianopic field defects (monocular)
1	5.26%	−21.05%	90	115	Annular scotomata
2	−11.58%	−25.26%	106	119	Generally reduced light-difference-sensitivity
20	−29.47%	−43.16%	123	136	Nerve fibre bundle defects: pseudo-conc. VF reduction
0	−64.21%	−96.84%	156	187	Concentric visual field reduction

- the *overlap parameter* q^{μ} defined as: $q^{\mu} := \frac{1}{N}\sum_{i=1}^{N}\sigma_i\sigma_i^{\mu}$
- the *Hamming distance* H^{μ} defined as: $H^{\mu} := N - \sum_{i=1}^{N}\delta_{\sigma_i\sigma_i^{\mu}}$

with $\vec{\sigma}$ being the scotomata pattern derived from the perimetric examination and $\vec{\sigma}^{\mu}$ being the μth idealized scotomata attractor. To enable a comparison/analysis, the overlap parameter and the Hamming distance are calculated, for all possible pairs of examination result and network attractors, before and after the above-described relaxation process. Table 1 shows a classification example of the visual field data depicted in figures 3–5: from the definition of the overlap parameter and the Hamming distance follows that the attractor with the largest overlap (closest to 1 or 100%) and the smallest Hamming distance (closest to 0; the worst/largest Hamming distance would be N) classifies the scotomata pattern under examination best (in this case a centrocoecal visual field defect, visual field defect code VFDC = 21).

3. Results

Preliminary tests of the classification system on *real* monocular visual field data derived from perimetric examinations, performed with the TAP, have shown a classification success of about 80% (Fink *et al* 1999), which is well in line with, e.g., about 74% reported in Goldbaum *et al* (1994) and 65–100% on genuine field results reported in Mutlukan and Keating (1994). In section 4 various approaches are outlined that would potentially yield an improvement in the success rate in future versions of the classification system. Further application of the Hopfield-

attractor network-classification method in a clinical setting in collaboration with visual field experts is certainly necessary but beyond the scope of this paper.

It should be mentioned that the classification result and, therefore, the classification success depend on the choice of the previously introduced user-/examination-defined luminosity class threshold that is used for the conversion of the initial perimetric examination result to a binary pattern: if the threshold is set to the lowest luminosity class, then all 190 test locations will indicate an absolute scotoma (indicating a blind central visual field), thus rendering a classification meaningless. Conversely, a luminosity class threshold set to the highest luminosity class will always result in a 'normal' diagnosis, regardless of the scotomata encountered. Therefore, the luminosity class threshold has to be chosen carefully between the two extrema. Unless not otherwise motivated, the luminosity class threshold can be subject to optimization to improve on the overall classification success rate (see section 4). For the results reported here, the luminosity class threshold was set to the second lowest luminosity class out of a total of seven used by the Tübingen Automated Perimeter.

The main advantages of the proposed Hopfield-attractor-network-based approach over feed-forward type neural networks are:

- The network architecture is defined by the classification problem alone, as opposed to the somewhat arbitrary choice of both the number of hidden layers and the number of neurons per hidden layer in feed-forward type neural networks.
- No neural learning process is required for determining the synaptic coupling strengths for the neural network for classification of visual field data as opposed to learning algorithms, necessary for the training of feed-forward type neural nets, such as *error-backpropagation* (Rumelhart *et al* 1986a, 1986b). In addition, the size and diversity of the training set, necessary for learning the coupling strengths of a real-world (finite) feed-forward net for a given classification task, is not known *a priori*. Furthermore, changes in the training set usually require retraining of the coupling strengths of a feed-forward neural net as opposed to an almost instant recalculation in the case of a Hopfield-attractor network.
- Even early stages of an ophthalmological or neuroophthalmological disease may eventually be classified correctly (see figures 3–5) according to the predefined attractors of the network, thanks to its dynamic, iterative relaxation process, which enables the Hopfield–attractor network to classify even 'noisy' input patterns. A feed-forward type neural network performs by definition only one pass-through.
- The assignment of a confidence level to the diagnosis, e.g., by means of the overlap parameter and the Hamming distance, makes the system a more realistic 'counsellor' rather than just a 'yes/no-machine'.

The proposed Hopfield–attractor-network-based classification system may be readily applied to arbitrary stimulus grids for static perimetry (e.g., 30°-, 90°-visual fields and Humphrey visual fields, etc), since only the idealized scotomata patterns (network attractors) have to be adjusted accordingly. Thus, the TAP stimulus grid for a 30°-visual field, used in this study, is only one instantiation of possible stimulus grid arrangements, and, with its 191 (eccentric + centre) test locations, it allows for a high spatial resolution of position, shape and extent of scotomata (compared to only 60–70 test locations of conventional automated threshold perimetry).

4. Discussion and outlook

Future developments of the attractor-network classification system currently pursued comprise the following:

- Optimization of the classification success by varying the luminosity class threshold used for the conversion of the initial perimetric examination result to a binary pattern for subsequent classification by the Hopfield-attractor network.
- Implementation of stimulus grids other than the Tübingen Automated Perimeter stimulus grid for various visual fields (e.g., 30°-, 90°-visual fields and Humphrey visual fields, etc.).
- Adjustment of the idealized scotomata pattern set to these other stimulus grids.
- Continued research in the detailed specification of the network attractor sets (idealized scotomata patterns) to allow for more precise and specific classifications.
- Iterated diagnosis process through the assignment of a separate neural network to each disease respectively, which has been pre-classified by the classification system with a high confidence level, e.g., a network that is specialized in the various scotomata patterns caused by glaucoma, only.
- Expansion of the Hopfield-attractor network formalism from a binary (*Ising spin*) system to an *N*-state (*Potts spin*) system per neuron (*N-state Potts model*/*Potts spin glass*, e.g., Wu (1983) and Müller and Reinhardt (1990)), in order to take into account relative scotomata, i.e. all available tested luminosity classes (7 for the Tübingen Automated Perimeter). This would render the luminosity class threshold-based conversion unnecessary.
- Consideration of binocular visual field data for diagnosis of binocular scotomata.
- Exploration and use of existing correlations between the perimetric examination results of left and right eye.
- Taking into consideration the temporal progress of various ophthalmological and neuroopthalmological diseases that can be monitored by means of perimetric examinations.

Since we are at the beginning of a new era of computer-based classification systems in medical sciences, one should not be too restrictive in choosing the appropriate neural network type. Rather, combinations of different neural network types should also be considered, such as feed-forward nets, attractor networks and/or self-organizing (Kohonen) maps.

The novel method for computer-based classification of visual field data, presented here, furnishes a valuable first overview in judging perimetric examination results, pointing towards a final diagnosis by a physician. It should not be considered a substitute for the diagnosing physician, but may rather act as a 'counsellor', providing an independent 'second opinion', thereby potentially increasing the diagnosis accuracy and reducing the risk for error. Further, the potential for recognizing early stages of ophthalmological and neuroophthalmological diseases offers the opportunity for early/timely treatment, essential for diseases such as glaucoma.

Finally, we would like to mention that an Internet-based experimental version of the classification system (Fink 1999) is publicly accessible at http://www.wfbabcom5.com/wf33.htm. Thanks to the worldwide accessibility of the Internet, the classification system offers a promising perspective towards modern computer-assisted diagnosis in both medicine and tele-medicine, for example and in particular, with respect to non-ophthalmic clinics or in communities where perimetric expertise is not readily available.

Acknowledgment

I would like to thank E W Schmid for scientific advice and valuable discussions.

References

Brigatti L, Nouri Mahdavi K, Weitzman M and Caprioli J 1997 Automatic detection of glaucomatous visual field progression with neural networks *Arch. Ophthalmol.* **115** 725–8

Fink W 1999 Internet-based neural network classification of visual field data *Invest. Ophthalmol. Vis. Sci.* **40** 657

Fink W, Schiefer U and Schmid E W 1999 Neural attractor network classification of visual field data *Proc. 13th Int. Perimetric Society Meeting (Gardone Riviera (BS) 6–9 Sept. 1998)* ed M Wall and J M Wild (The Hague: Kugler) pp 283–8 (Perimetry update 1998/1999)

Goldbaum M H, Sample P A, White H, Côlt B, Raphaelian P, Fechtner R D and Weinreb R N 1994 Interpretation of automated perimetry for glaucoma by neural network *Invest. Ophthalmol. Vis. Sci.* **35** 3362–73

Henson D B, Spenceley S and Bull D R 1996 Spatial classification of glaucomatous visual field loss *Br. J. Ophthalmol.* **80** 526–31

Henson D B, Spenceley S and Bull D R 1997a Fieldnet: package for the spatial classification of glaucomatous visual field defects *Proc. 12th Int. Perimetric Society Meeting (Würzburg 4–8 June 1996)* ed M Wall and A Heijl (Amsterdam: Kugler) pp 289–98 (Perimetry update 1996/1997)

Henson D B, Spenceley S and Bull D R 1997b Artificial neural network analysis of noisy visual field data in glaucoma *Artif. Intell. Med.* **10** 99–113

Hertz J, Krogh A and Palmer R G 1991 *Introduction to the Theory of Neural Computation (Lecture Notes* vol 1*)* (Reading, MA: Addison-Wesley)

Hopfield J J 1982 Neural networks and physical systems with emergent collective computational abilities *Proc. Natl. Acad. Sci. USA* **79** 2554–8

Keating D, Mutlukan E, Damato B and Evans A 1992 A back propagation neural network for the classification of visual field data *Invest. Ophthalmol. Vis. Sci.* **33** 970

Keating D, Mutlukan E, Evans A, McGaryle J and Damato B 1993 A back propagation neural network for the classification of visual field data *Phys. Med. Biol.* **38** 1263–70

Kelman S E, Perell H F, D'Autrechy L and Scott R J 1991 A neural network can differentiate glaucoma and optic neuropathy visual fields through pattern recognition *Proc. 9th Int. Perimetric Society Meeting (Malmö, 17–20 June 1990)* ed R P Mills and A Heijl (Amsterdam: Kugler) pp 287–90 (Perimetry update 1990/1991)

Müller B and Reinhardt J 1990 *Neural Networks: An Introduction* (Berlin: Springer)

Mutlukan E and Keating D 1994 Visual field interpretation with a personal computer based neural network *Eye* **8** 321–3

Nagata S, Kani K and Sugiyama A 1991 A computer–assisted visual field diagnosis system using a neural network *Proc. 9th Int. Perimetric Society Meeting (Malmö 17–20 June 1990)* ed R P Mills and A Heijl (Amsterdam: Kugler) pp 291–5 (Perimetry update 1990/1991)

Schiefer U and Wilhelm H 1995 Gesichtsfeld–Kompendium. Interpretation perimetrischer Befunde. Fachübergreifende diagnostische Maßnahmen *Klin. Monatsbl. Augenheilkd.* **206** 206–38

Spenceley S, Henson D B and Bull D R 1994 Visual field analysis using artificial neural networks *Ophthalmic. Physiol. Opt.* **14** 239–48

Rumelhart D E, Hinton G E and Williams R J 1986a Learning representations by back-propagating errors *Nature* **323** 533–6

Rumelhart D E, Hinton G E and Williams R J 1986b Learning internal representations by error propagation *Parallel Distributed Processing* ed D E Rumelhart and J L McClelland (Cambridge: MIT Press)

Wu F Y 1983 The Potts model *Rev. Mod. Phys.* **54** 235